Dynamics and Control of Spacecraft with Retargeting Flexible Antennas

Leonard Meirovitch* and Moon K. Kwak†
Virginia Polytechnic Institute and State University, Blacksburg, Virginia

This investigation is concerned with the dynamics and control of a spacecraft comprising a rigid platform and a given number of retargeting flexible antennas. The mission consists of maneuvering the antennas so as to coincide with preselected lines of sight while stabilizing the platform in an inertial space and suppressing the elastic vibration of the antennas. The paper contains the derivation of the equations of motion by a Lagrangian approach using quasicoordinates, as well as a procedure for designing the feedback controls. A numerical example involving a spacecraft consisting of a rigid platform and a flexible antenna is presented.

I. Introduction

In many space applications, it becomes necessary to reorient a certain line of sight in a spacecraft. Examples of this are the reorientation relative to an inertial space of a space telescope or of an antenna in a spacecraft. In some cases, such as the space telescope, this amounts to reorientation of the entire spacecraft. Many spacecraft can be represented by mathematical models consisting of a rigid platform with one or several flexible appendages, such as flexible antennas, so that the mission involves the maneuvering of a hybrid system.[1-5]

Quite often, however, the line of sight coincides with an axis fixed in an antenna, in which case it may be more advisable to retarget only the antenna and not the entire spacecraft. This is particularly true when the inertia of the antenna is much smaller than the inertia of the spacecraft. The argument becomes even stronger when several antennas must be retargeted, and each one must be reoriented into a different direction in space. In such cases, it appears more sensible to conceive of a spacecraft consisting of a rigid platform stabilized in an inertial space and several appendages, rigid or flexible, hinged to the platform and capable of pivoting about two orthogonal axes relative to the platform. In this case, reorientation relative to the stabilized platform is equivalent to retargeting in an inertial space. This paper is concerned with retargeting of flexible antennas.

Figure 1 shows a spacecraft comprising a rigid platform and a given number of flexible appendages. Assuming that the flexible appendages represent antennas, the mission consists of maneuvering the antennas so as to coincide with preselected lines of sight. Of course, because the system linear and angular momenta are conserved in the absence of external forces and torques, reorientation of the antennas will cause perturbations in the platform. Hence, the mission design can be regarded as involving several interdependent tasks. The first task is to select and implement policies for the maneuvering of the antennas relative to the inertial space. The second consists of stabilizing the attitude and position of the platform relative to the inertial space. The third task is simply to suppress any vibration of the flexible antennas caused by the maneuver. Of course, maneuvering of the antennas, stabilization of the platform, and vibration suppression are to take place simultaneously.

The motion of the spacecraft is conveniently described by six ordinary differential equations for the three rigid-body translations and rotations of the platform, and by partial differential equations for the elastic deformations of each antenna. For practical reasons, the latter are transformed into sets of ordinary differential equations, thus reducing the control problem to a regulator problem. This is no ordinary regulator problem, however, as the maneuvering of the flexible antennas relative to the platform induces time-dependent coefficients.

Under certain circumstances, the time-varying terms are sufficiently small that they can be ignored in the control design.

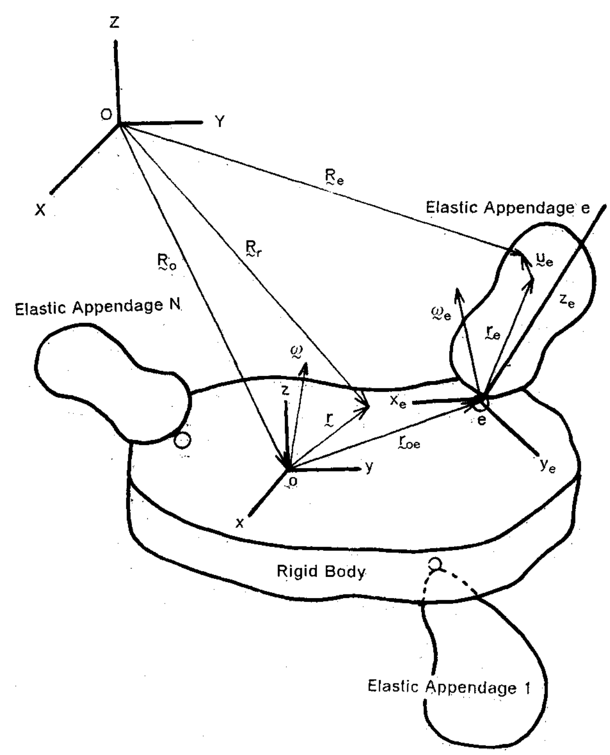

Fig. 1 Mathematical model of the spacecraft.

Presented as Paper 88-2414 at the AIAA/ASME/AHS 29th Structures, Structural Dynamics, and Materials Conference, Williamsburg, VA, April 18-20, 1988; received May 13, 1988; revision received Aug. 29, 1988. Copyright © 1988 American Institute of Aeronautics and Astronautics, Inc. All rights reserved.

*University Distinguished Professor, Department of Engineering Science and Mechanics. Fellow AIAA.

†Graduate Research Assistant; currently, Assistant Professor, Department of Engineering Science and Mechanics. Student Member AIAA.

Even then, however, the full time-varying system must be considered in implementing the feedback controls designed on the basis of the time-invariant system.

This paper contains the derivation of the equations of motion for the spacecraft just described, as well as the procedure for designing the feedback controls. The equations of motion were derived by a Lagrangian approach using quasicoordinates,[6] and optimal control gains were obtained by using a quadratic performance measure.[7] The approach is demonstrated by means of a numerical example involving a spacecraft consisting of a rigid platform and a single flexible antenna. The antenna undergoes a 45-deg reorientation relative to the platform while the platform is being stabilized relative to an inertial space and the vibration of the antenna is being suppressed.

II. Derivation of the Equations of Motion

Let us consider a spacecraft consisting of a rigid platform and a given number of flexible antennas hinged to the platform. The object is to retarget the flexible antennas so as to point in different directions in an inertial space. The strategy consists of stabilizing the rigid platform relative to the inertial space and maneuvering the flexible antennas relative to the platform. In this section, we propose to derive the equations of motion capable of describing this task. To this end, we use a new formulation of Lagrange's equations for flexible bodies in terms of quasicoordinates.[6]

To describe the motion, we introduce a set of inertial axes XYZ with the origin at 0, a set of body axes xyz coinciding with the principal axes of the rigid platform and with the origin at the mass center o of the platform, and sets of body axes $x_e y_e z_e$ embedded in the elastic appendages in undeformed state and with the origin at the hinge points $(e=1,2,\ldots,N)$. The body and the various axes are shown in Fig. 1. The position vector of a point in the rigid body and a typical flexible appendage can be written as $\boldsymbol{R}_r = \boldsymbol{R}_o + \boldsymbol{r}$ and $\boldsymbol{R}_e = \boldsymbol{R}_o + \boldsymbol{r}_{oe} + \boldsymbol{r}_e + \boldsymbol{u}_e$ $(e=1,2,\ldots,N)$, respectively, where $\boldsymbol{R}_o$ is the radius vector from 0 to o, $\boldsymbol{r}$ is the position vector of a point in the rigid body relative to o, $\boldsymbol{r}_{oe}$ is the radius vector from o to e, $\boldsymbol{r}_e$ the nominal position vector of a point in the undeformed appendage e, and $\boldsymbol{u}_e$ is the elastic displacement vector of that point. We note that vector $\boldsymbol{R}_o$ is given in terms of components along XYZ, $\boldsymbol{r}$ and $\boldsymbol{r}_{oe}$ in terms of components along xyz, and $\boldsymbol{r}_e$ and $\boldsymbol{u}_e$ in terms of components along $x_e y_e z_e$. We assume that axes xyz rotate with the angular velocity ω relative to the inertial space, and that $x_e y_e z_e$ rotate with the angular velocity ω_e relative to axes xyz, where ω is in terms of components along xyz, and ω_e is in terms of components along $x_e y_e z_e$. Thus, denoting by E_e the matrix of direction cosines between axes $x_e y_e z_e$ and xyz, the velocity vector of a point on the rigid body and one on a typical elastic appendage can be expressed as

$$\dot{\boldsymbol{R}}_r = \boldsymbol{V}_o + \omega \times \boldsymbol{r} \tag{1a}$$

$$\dot{\boldsymbol{R}}_e = E_e(\boldsymbol{V}_o + \omega \times \boldsymbol{r}_{oe}) + (E_e\omega + \omega_e) \times (\boldsymbol{r}_e + \boldsymbol{u}_e) + \boldsymbol{v}_e \qquad e = 1,2,\ldots,N \tag{1b}$$

where $\boldsymbol{V}_o$ is the velocity of o in terms of components along axes xyz and $\boldsymbol{v}_e$ is the elastic velocity vector of a point on the appendage e as measured relative to axes $x_e y_e z_e$. Note that $\dot{\boldsymbol{R}}_r$ is in terms of components along xyz and $\dot{\boldsymbol{R}}_e$ in terms of components along $x_e y_e z_e$. We also note that

$$\boldsymbol{V}_o = C\dot{\boldsymbol{R}}_o \tag{2a}$$

$$\omega = D\dot{\theta} \tag{2b}$$

$$\boldsymbol{v}_e = \dot{\boldsymbol{u}}_e, \qquad e = 1,2,\ldots,N \tag{2c}$$

in which, for the particular choice of angular displacements shown in Fig. 2,

$$C = \begin{bmatrix} c\theta_2 c\theta_3 & c\theta_1 s\theta_3 + s\theta_1 s\theta_2 c\theta_3 & s\theta_1 s\theta_3 - c\theta_1 s\theta_2 c\theta_3 \\ -c\theta_2 s\theta_3 & c\theta_1 c\theta_3 - s\theta_1 s\theta_2 s\theta_3 & s\theta_1 c\theta_3 + c\theta_1 s\theta_2 s\theta_3 \\ s\theta_2 & -s\theta_1 c\theta_2 & c\theta_1 c\theta_2 \end{bmatrix} \tag{3a}$$

$$D = \begin{bmatrix} c\theta_2 c\theta_3 & s\theta_3 & 0 \\ -c\theta_2 s\theta_3 & c\theta_3 & 0 \\ s\theta_2 & 0 & 1 \end{bmatrix} \tag{3b}$$

where $s\theta_i = \sin\theta_i$ and $c\theta_i = \cos\theta_i$ $(i=1,2,3)$. We observe that C is a rotation matrix permitting us to express the velocity vector of point o on the rigid platform in terms of components along xyz and $\dot{\theta}$ is a vector of angular velocity components representing time derivatives of the angles θ_1, θ_2, and θ_3, as opposed to ω whose components can be interpreted as time derivatives of quasicoordinates.[6]

Because the maneuver angular velocities ω_e are given, the unknown motions are defined by the rigid-body motions $\boldsymbol{V}_o$ and ω and the elastic motions $\boldsymbol{u}_e$ $(e=1,2,\ldots,N)$. Hence, Lagrange's equations in terms of quasicoordinates consist of the hybrid set[6]

$$\frac{\mathrm{d}}{\mathrm{d}t}\left(\frac{\partial L}{\partial \boldsymbol{V}_o}\right) + \tilde{\omega}\left(\frac{\partial L}{\partial \boldsymbol{V}_o}\right) - C\left(\frac{\partial L}{\partial \boldsymbol{R}_o}\right) = \boldsymbol{F} \tag{4a}$$

$$\frac{\mathrm{d}}{\mathrm{d}t}\left(\frac{\partial \hat{L}}{\partial \omega}\right) + \tilde{V}_o\frac{\partial L}{\partial \boldsymbol{V}_o} + \tilde{\omega}\frac{\partial L}{\partial \omega} - (D^T)^{-1}\frac{\partial L}{\partial \theta} = \boldsymbol{M} \tag{4b}$$

$$\frac{\partial}{\partial t}\left(\frac{\partial \hat{L}_e}{\partial \boldsymbol{v}_e}\right) - \frac{\partial \hat{T}_e}{\partial \boldsymbol{u}_e} - \mathcal{L}_e \boldsymbol{u}_e = \hat{U}_e, \qquad e = 1,2,\ldots,N \tag{4c}$$

where $L = T - V$ is the Lagrangian in which T is the kinetic energy and V is the potential energy, $\hat{L}_e$ is the Lagrangian density and $\hat{T}_e$ the kinetic energy density for appendage e, and $\mathcal{L}_e$ is a matrix of homogeneous differential operators. Moreover, $\boldsymbol{F}$ and $\boldsymbol{M}$ are nonconservative force and torque vectors associated with the rigid-body motions of the spacecraft, both expressed in terms of components along xyz, and $\hat{U}_e$ $(e=1,2,\ldots N)$ are nonconservative force densities associated with the appendages and are given in terms of components

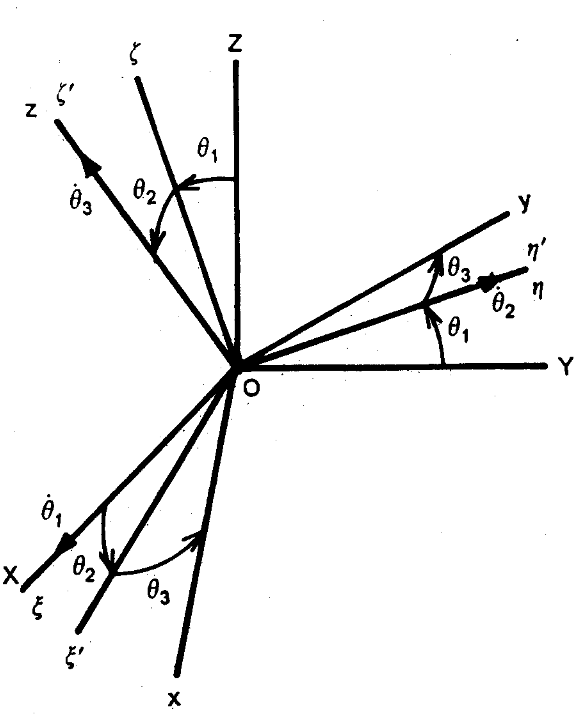

Fig. 2 Angular displacements and velocities of the rigid platform.

along $x_e y_e z_e$. Equations (4) are hybrid in the sense that Eqs. (4a) and (4b) are ordinary differential equations and Eqs. (4c) are partial differential equations. It should be noted that the tilde over a symbol indicates a skew symmetric matrix with entries corresponding to the components of the associated vector.[6] The displacement vectors $\boldsymbol{u}_e$ are subject to given boundary conditions.

Control design in terms of hybrid differential equations is not feasible, so that we must resort to discretization in space of the partial differential equations. To this end, we let the elastic displacement vector of a given point of appendage e have the form

$$\boldsymbol{u}_e(\boldsymbol{r}_e,t) = \Phi_e(\boldsymbol{r}_e)\boldsymbol{q}_e(t) \tag{5}$$

where Φ_e is a matrix of admissible functions[8] and $\boldsymbol{q}_e$ is a vector of generalized coordinates. Equation (5) permits us to replace the partial differential equations [Eq. (4c)] by the ordinary differential equations

$$\frac{\mathrm{d}}{\mathrm{d}t}\left(\frac{\partial L}{\partial \dot{\boldsymbol{q}}_e}\right) - \frac{\partial L}{\partial \boldsymbol{q}_e} = \boldsymbol{Q}_e, \qquad e = 1,2,\ldots,N \tag{6}$$

where

$$\boldsymbol{Q}_e = \int_{D_e} \Phi_e^T \hat{\boldsymbol{U}}_e \,\mathrm{d}D_e, \qquad e = 1,2,\ldots,N \tag{7}$$

Next, we propose to derive the system equations of motion using Eqs. (4a), (4b), and (6). To this end, we must derive expressions for the Lagrangian, which involves the kinetic energy and the potential energy, and the virtual work of the nonconservative forces. Using Eqs. (1), the kinetic energy can be written as

$$\begin{aligned} T &= \frac{1}{2}\int_{m_r} \dot{\boldsymbol{R}}_r^T \dot{\boldsymbol{R}}_r \,\mathrm{d}m_r + \frac{1}{2}\sum_{e=1}^{N} \int_{m_e} \dot{\boldsymbol{R}}_e^T \dot{\boldsymbol{R}}_e \,\mathrm{d}m_e \\ &= \frac{1}{2} m_t \boldsymbol{V}_o^T \boldsymbol{V}_o + \boldsymbol{V}_o^T \tilde{S}_t^T \boldsymbol{\omega} + \frac{1}{2}\boldsymbol{\omega}^T I_t \boldsymbol{\omega} + \frac{1}{2}\sum_{e=1}^{N} \boldsymbol{\omega}_e^T I_e \boldsymbol{\omega}_e \\ &+ \boldsymbol{V}_o^T \sum_{e=1}^{N} E_e^T \tilde{S}_e^T \boldsymbol{\omega}_e + \boldsymbol{\omega}^T \sum_{e=1}^{N} (\tilde{r}_{oe} E_e^T \tilde{S}_e^T + E_e^T I_e)\boldsymbol{\omega}_e \\ &+ \frac{1}{2}\sum_{e=1}^{N} \dot{\boldsymbol{q}}_e^T M_e \dot{\boldsymbol{q}}_e - \frac{1}{2}\sum_{e=1}^{N} \boldsymbol{q}_e^T \bar{H}_e(\boldsymbol{\omega}_e)\boldsymbol{q}_e + \boldsymbol{V}_o^T \sum_{e=1}^{N} E_e^T \bar{\Phi}_e \dot{\boldsymbol{q}}_e \\ &+ \boldsymbol{V}_o^T \sum_{e=1}^{N} E_e^T \tilde{\omega}_e \bar{\Phi}_e \boldsymbol{q}_e + \boldsymbol{\omega}^T \sum_{e=1}^{N} \tilde{r}_{oe} E_e^T \bar{\Phi}_e \dot{\boldsymbol{q}}_e \\ &+ \boldsymbol{\omega}^T \sum_{e=1}^{N} \tilde{r}_{oe} E_e^T \tilde{\omega}_e \bar{\Phi}_e \boldsymbol{q}_e + \sum_{e=1}^{N} \dot{\boldsymbol{q}}_e^T \tilde{\bar{\Phi}}_e^T E_e \boldsymbol{\omega} + \sum_{e=1}^{N} \dot{\boldsymbol{q}}_e^T \tilde{\bar{\Phi}}_e^T \boldsymbol{\omega}_e \\ &+ \sum_{e=1}^{N} \dot{\boldsymbol{q}}_e^T \tilde{H}_e(\boldsymbol{\omega}_e)\boldsymbol{q}_e + \boldsymbol{\omega}^T \sum_{e=1}^{N} E_e^T J_e(\boldsymbol{\omega}_e)\boldsymbol{q}_e \\ &+ \sum_{e=1}^{N} \boldsymbol{\omega}_e^T \left(\int_{m_e} \tilde{r}_e \tilde{\omega}_e \Phi_e \,\mathrm{d}m_e\right)\boldsymbol{q}_e \end{aligned} \tag{8}$$

where we note that, assuming small elastic motions, terms of order higher than two involving the elastic displacements have been neglected. Because the rigid-body motions of the platform are caused by the motion of the appendages, whose inertia is small relative to the inertia of the platform, the rigid-body motions are also sufficiently small that terms of order higher than two in these motions can be ignored. The various quantities entering into Eq. (8) are as follows:

$$m_t = m_r + \sum_{e=1}^{N} m_e \tag{9a}$$

$$I_t = I_r + \sum_{e=1}^{N} (m_e \tilde{r}_{oe} \tilde{r}_{oe}^T + E_e^T I_e E_e + \tilde{r}_{oe}^T E_e^T \tilde{S}_e E_e + E_e^T \tilde{S}_e^T E_e \tilde{r}_{oe}) \tag{9b}$$

$$\tilde{S}_t = \sum_{e=1}^{N} (m_e \tilde{r}_{oe} + E_e^T \tilde{S}_e E_e) \tag{9c}$$

$$S_e = \int_{m_e} \boldsymbol{r}_e \,\mathrm{d}m_e \tag{9d}$$

$$I_r = \int_{m_r} \tilde{r}\tilde{r}^T \,\mathrm{d}m_r \tag{9e}$$

$$I_e = \int_{m_e} \tilde{r}_e \tilde{r}_e^T \,\mathrm{d}m_e \tag{9f}$$

$$M_e = \int_{m_e} \Phi_e^T \Phi_e \,\mathrm{d}m_e \tag{9g}$$

$$\bar{\Phi}_e = \int_{m_e} \Phi_e \,\mathrm{d}m_e \tag{9h}$$

$$\tilde{\bar{\Phi}}_e = \int_{m_e} \tilde{r}_e \Phi_e \,\mathrm{d}m_e \tag{9i}$$

$$\tilde{H}_e(\boldsymbol{\omega}_e) = \int_{m_e} \Phi_e^T \tilde{\omega}_e \Phi_e \,\mathrm{d}m_e \tag{9j}$$

$$\bar{H}_e(\boldsymbol{\omega}_e) = \int_{m_e} \Phi^T \tilde{\omega}_e^2 \Phi_e \,\mathrm{d}m_e \tag{9k}$$

$$J_e(\boldsymbol{\omega}_e) = \int_{m_e} [\tilde{r}_e \tilde{\omega}_e + \widetilde{(r_e \omega_e)}]\Phi_e \,\mathrm{dm_e} \tag{9l}$$

Similarly, the potential energy has the expression

$$V = \frac{1}{2}\sum_{e=1}^{N} [\boldsymbol{u}_e,\boldsymbol{u}_e] = \frac{1}{2}\sum_{e=1}^{N} \boldsymbol{q}_e^T [\Phi_e,\Phi_e]\boldsymbol{q}_e = \frac{1}{2}\sum_{e=1}^{N} \boldsymbol{q}_e^T K_e \boldsymbol{q}_e \tag{10}$$

where $K_e = [\Phi_e, \Phi_e]$, in which the symbol [,] represents an energy inner product.[8]

Before deriving explicit equations of motion, it is advisable to express the generalized forces appearing on the right side of Eqs. (4a), (4b), and (6) in terms of actual forces. To this end, we denote by $\boldsymbol{F}_o$ the actuator force and by $\boldsymbol{M}_o$ the actuator torque acting on the platform. In addition, every appendage e is subjected to a distributed actuator force vector $\boldsymbol{f}_e$. The vectors $\boldsymbol{F}_o$ and $\boldsymbol{M}_o$ are in terms of components along xyz, and the vectors $\boldsymbol{f}_e$ are in terms of components along $x_e y_e z_e$. In writing the virtual work, we propose to express all vectors in terms of components along xyz. Consistent with this, we write the distributed force in the form

$$\boldsymbol{f}_e^* = E_e^T \boldsymbol{f}_e, \qquad e = 1,2,\ldots,N \tag{11}$$

where E_e is the matrix of direction cosines defined earlier. Moreover, the virtual displacement associated with a point on appendage e can be written in terms of components along xyz as

$$\delta\boldsymbol{R}_e = \delta\boldsymbol{R}_o^* - [\tilde{r}_{oe} + \widetilde{(E_e^T \boldsymbol{r}_e)}]\,\delta\boldsymbol{\theta}^* + E_e^T \delta\boldsymbol{u}_e \tag{12}$$

where $\delta\boldsymbol{R}_o^*$ and $\delta\boldsymbol{\theta}^*$ can be identified as virtual quasidisplacement vectors. Hence, considering Eqs. (1b), (11), and (12), recalling that $\boldsymbol{\omega}_e$ is a given quantity and ignoring second-order effects, the virtual work in terms of actual forces can be written in the form

$$\begin{aligned} \delta W &= \boldsymbol{F}_o^T \delta\boldsymbol{R}_o^* + \boldsymbol{M}_o^T \delta\boldsymbol{\theta}^* + \sum_{e=1}^{N} \int_{D_e} (\boldsymbol{f}_e^*)^T \delta\boldsymbol{R}_e \,\mathrm{d}D_e \\ &= \boldsymbol{F}_o^T \delta\boldsymbol{R}_o^* + \boldsymbol{M}_o^T \delta\boldsymbol{\theta}^* + \sum_{e=1}^{N} \int_{D_e} \boldsymbol{f}_e^T E_e \{\delta\boldsymbol{R}_o^* \\ &- [\tilde{r}_{oe} + \widetilde{(E_e^T \boldsymbol{r}_e)}]\delta\boldsymbol{\theta}^* + E_e^T \delta\boldsymbol{u}_e\} \,\mathrm{d}D_e = \boldsymbol{F}^T \delta\boldsymbol{R}_o^* \\ &+ \boldsymbol{M}^T \delta\boldsymbol{\theta}^* + \sum_{e=1}^{N} \int_{D_e} \boldsymbol{f}_e^T \delta\boldsymbol{u}_e \,\mathrm{d}D_e \end{aligned} \tag{13}$$

where

$$F = F_o + \sum_{e=1}^{N} \int_{D_e} E_e^T f_e \, dD_e \tag{14a}$$

$$M = M_o + \sum_{e=1}^{N} \int_{D_e} (\tilde{r}_{oe} + \widetilde{E_e^T r_e}) E_e^T f_e \, dD_e \tag{14b}$$

Moreover, from Eq. (13) we conclude that

$$\hat{U}_e = f_e \tag{15}$$

so that, using Eqs. (7),

$$Q_e = \int_{D_e} \Phi_e^T f_e \, dD_e, \qquad e = 1,2,\ldots,N \tag{16}$$

In practice, we use point actuators instead of distributed ones. But, discrete forces can be regarded as distributed by writing

$$f_e = \sum_{i=1}^{n_e} F_{ei}\delta(r_e - r_{ei}), \qquad e = 1,2,\ldots,N \tag{17}$$

where F_{ei} are time-dependent force amplitudes and $\delta(r_e - r_{ei})$ are spatial Dirac delta functions. Inserting Eqs. (17) into Eq. (16), we obtain

$$Q_e = \int_{D_e} \Phi_e^T \sum_{e=1}^{n_e} F_{ei}\delta(r_e - r_{ei}) \, dD_e = \sum_{e=1}^{n_e} \Phi_e^T(r_{ei})F_{ei}, \qquad e = 1,2,\ldots,N \tag{18}$$

The equations of motion are obtained by inserting Eqs. (8), (10), (14), and (18) into Eqs. (4a), (4b), and (6). The result is

$$m_t \dot{V}_o + \tilde{S}_t^T \dot{\omega} + 2\sum_{e=1}^{N} E_e^T (\widetilde{S_e \omega_e}) E_e \omega + \sum_{e=1}^{N} E_e^T \bar{\Phi}_e \ddot{q}_e + 2\sum_{e=1}^{N} E_e^T \tilde{\omega}_e \bar{\Phi}_e \dot{q}_e + \sum_{e=1}^{N} E_e^T(\dot{\tilde{\omega}}_e + \tilde{\omega}_e^2)\bar{\Phi}_e q_e = F_o + \sum_{e=1}^{N}\sum_{i=1}^{n_e} E_e^T F_{ei} + \sum_{e=1}^{N} E_e^T(\tilde{S}_e \dot{\omega}_e + \tilde{\omega}_e \tilde{S}_e \omega_e) \tag{19a}$$

$$\tilde{S}_t \dot{V}_o + I_t \dot{\omega} + \sum_{e=1}^{N} [E_e^T(2\tilde{\omega}_e I_e - \text{tr} I_e \tilde{\omega}_e)E_e + 2\tilde{r}_{oe} E_e^T (\widetilde{S_e \omega_e}) E_e]\omega + \sum_{e=1}^{N} (E_e^T \tilde{\Phi}_e + \tilde{r}_{oe} E_e^T \bar{\Phi}_e)\ddot{q}_e + \sum_{e=1}^{N} [2\tilde{r}_{oe} E_e^T \tilde{\omega}_e \bar{\Phi}_e + E_e^T \tilde{\omega}_e \tilde{\Phi}_e + E_e^T J_e(\omega_e)]\dot{q}_e + \sum_{e=1}^{N} \{\tilde{r}_{oe} E_e^T (\tilde{\omega}_e^2 + \dot{\tilde{\omega}}_e)\bar{\Phi}_e + E_e^T[\tilde{\omega}_e J_e(\omega_e) + J_e(\dot{\omega}_e)]\} q_e = M_o + \sum_{e=1}^{N}\sum_{i=1}^{n_e} (\tilde{r}_{oe} E_e^T + E_e^T \tilde{r}_{ei})F_{ei} + \sum_{e=1}^{N} [\tilde{r}_{oe} E_e^T (\tilde{S}_e \dot{\omega}_e + \tilde{\omega}_e \tilde{S}_e \omega_e) - E_e^T(I_e \dot{\omega}_e + \tilde{\omega}_e I_e \omega_e)] \tag{19b}$$

$$\bar{\Phi}_e^T E_e \dot{V}_o + (\bar{\Phi}_e^T E_e \tilde{r}_{oe}^T + \tilde{\Phi}_e^T E_e)\dot{\omega} + [\bar{\Phi}_e^T \tilde{\omega}_e^T - J_e^T(\omega_e)]E_e \omega + M_e \ddot{q}_e + 2\tilde{H}_e(\omega_e)\dot{q}_e + [K_e + \bar{H}_e(\omega_e) + \tilde{H}_e(\dot{\omega}_e)]q_e = \sum_{i=1}^{n_e} \Phi_e^T(r_{ei})F_{ei} - \tilde{\Phi}_e^T \dot{\omega}_e + \int_{m_e} \Phi^T \omega_e \tilde{r}_e \omega_e \, dm_e, \qquad e = 1,2,\ldots,N \tag{19c}$$

At this point, we wish to cast the equations of motion in state form. The obtain the state equations, we adjoin Eqs. (2) to Eqs. (19). In view of the small motion assumption, as well as the spatial discretization, Eqs. (2) reduce to

$$V_o = \dot{R}_o \tag{20a}$$

$$\omega = \dot{\theta} \tag{20b}$$

$$p_e = \dot{q}_e, \qquad e = 1,2,\ldots,N \tag{20c}$$

where the notation is obvious. Introducing the state vector

$$x = [R_o^T \; \theta^T \; q_1^T \; q_2^T \ldots q_N^T \; V_o^T \; \omega^T \; p_1^T \; p_2^T \ldots p_N^T]^T \tag{21}$$

the state equations can be written in the compact matrix form

$$\dot{x}(t) = A(t)x(t) + B(t)f(t) + D(t)d(t) \tag{22}$$

in which

$$A(t) = \begin{bmatrix} 0 & I \\ -M^{-1}(t)K(t) & -M^{-1}(t)G(t) \end{bmatrix} \tag{23a}$$

$$B(t) = \begin{bmatrix} 0 \\ M^{-1}(t)B^*(t) \end{bmatrix} \tag{23b}$$

$$D(t) = \begin{bmatrix} 0 \\ M^{-1}(t) \end{bmatrix} \tag{23c}$$

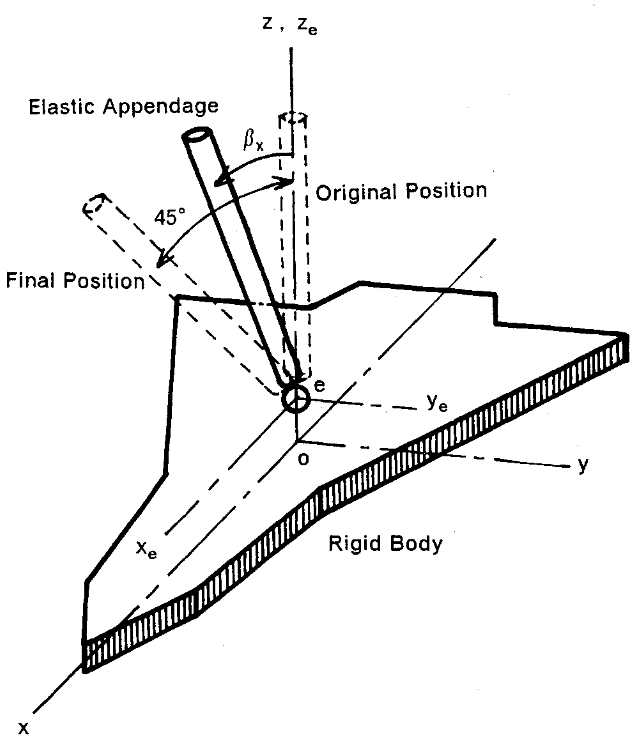

Fig. 3 The spacecraft with a single maneuvering flexible appendage.

where

$$M(t) = \begin{bmatrix} m_t I & \tilde{S}_t^T & E_1^T\bar{\Phi}_1 & \cdots & E_N^T\bar{\Phi}_N \\ \tilde{S}_t & I_t & E_1^T\tilde{\bar{\Phi}}_1 + \tilde{r}_{o1}E_1^T\bar{\Phi}_1 & \cdots & E_N^T\tilde{\bar{\Phi}}_N + \tilde{r}_{oN}E_N^T\bar{\Phi}_N \\ \bar{\Phi}_1^T E_1 & \tilde{\bar{\Phi}}_1^T E_1 + \bar{\Phi}_1^T E_1 \tilde{r}_{o1}^T & M_1 & \cdots & 0 \\ \cdot & \cdot & \cdot & \cdots & \cdot \\ \cdot & \cdot & \cdot & \cdots & \cdot \\ \bar{\Phi}_N^T E_N & \tilde{\bar{\Phi}}_N^T E_N + \bar{\Phi}_N^T E_N \tilde{r}_{oN}^T & 0 & \cdots & M_N \end{bmatrix} \tag{24a}$$

is a mass matrix,

$$K(t) = \begin{bmatrix} 0 & 0 & E_1^T(\tilde{\dot{\omega}}_1 + \tilde{\omega}_1^2)\bar{\Phi}_1 & \cdots & E_N^T(\tilde{\dot{\omega}}_N + \tilde{\omega}_N^2)\bar{\Phi}_N \\ 0 & 0 & \tilde{r}_{o1}E_1^T(\tilde{\omega}_1^2 + \tilde{\dot{\omega}}_1)\bar{\Phi}_1 + E_1^T[\tilde{\omega}_1 J_1(\omega_1) + J_1(\dot{\omega}_1)] & \cdots & \tilde{r}_{oN}E_N^T(\tilde{\omega}_N^2 + \tilde{\dot{\omega}}_N)\bar{\Phi}_N + E_N^T[\tilde{\omega}_N J_N(\omega_N) + J_N(\dot{\omega}_N)] \\ 0 & 0 & K_1 + \bar{H}_1(\omega_1) + \tilde{H}_1(\dot{\omega}_1) & \cdots & 0 \\ \cdot & \cdot & \cdot & \cdots & \cdot \\ \cdot & \cdot & \cdot & \cdots & \cdot \\ 0 & 0 & 0 & \cdots & K_N + \bar{H}_N(\omega_N) + \tilde{H}_N(\dot{\omega}_N) \end{bmatrix} \tag{24b}$$

plays the role of a stiffness matrix, and

$$G(t) = \begin{bmatrix} 0 & 2\sum_{e=1}^{N} E_e^T(\widetilde{\bar{S}_e\omega_e})E_e & 2E_1^T\tilde{\omega}_1\bar{\Phi}_1 & \cdots & 2E_N^T\tilde{\omega}_N\bar{\Phi}_N \\ 0 & G_{22} & G_{23}^1 & \cdots & G_{23}^N \\ 0 & [\tilde{\bar{\Phi}}_1^T\tilde{\omega}_1^T - J_1^T(\omega_1)]E_1 & 2\bar{H}_1(\omega_1) & \cdots & 0 \\ \cdot & \cdot & \cdot & \cdots & \cdot \\ \cdot & \cdot & \cdot & \cdots & \cdot \\ 0 & [\tilde{\bar{\Phi}}_N^T\tilde{\omega}_N^T - J_N^T(\omega_N)]E_N & 0 & \cdots & 2\bar{H}_N(\omega_N) \end{bmatrix} \tag{24c}$$

in which

$$G_{22} = \sum_{e=1}^{N}[E_e^T(2\tilde{\omega}_e I_e - \mathrm{tr} I_e\tilde{\omega}_e)E_e + 2\tilde{r}_{oe}E_e^T(\widetilde{\bar{S}_e\omega_e})E_e] \tag{25a}$$

$$G_{23}^e = 2\tilde{r}_{oe}E_e^T\tilde{\omega}_e\bar{\Phi}_e + E_e^T\tilde{\omega}_e\tilde{\bar{\Phi}}_e + E_e^T J_e(\omega_e) \tag{25b}$$

where tr denotes the trace of the matrix. Moreover,

$$B^*(t) = \begin{bmatrix} I & b^1 & b^2 & \cdots & b^N \\ 0 & c^1 & 0 & \cdots & 0 \\ 0 & 0 & c^2 & \cdots & 0 \\ \cdot & \cdot & \cdot & \cdots & \cdot \\ \cdot & \cdot & \cdot & \cdots & \cdot \\ 0 & 0 & 0 & \cdots & c^N \end{bmatrix} \tag{26}$$

is a matrix relating the discrete force vectors to the modal vectors, where

$$b^e = \begin{bmatrix} E_e^T & E_e^T & \cdots & E_e^T \\ \tilde{r}_{oe}E_e^T + E_e^T\tilde{r}_{e1} & \tilde{r}_{oe}E_e^T + E_e^T\tilde{r}_{e2} & \cdots & \tilde{r}_{oe}E_e^T + E_e^T\tilde{r}_{en_e} \end{bmatrix} \tag{27a}$$

$$c^e = [\Phi_e^T(r_{e1}) \quad \Phi_e^T(r_{e2}) \quad \cdots \quad \Phi_e^T(r_{en_e})] \tag{27b}$$

Finally,

$$f = [F_o^T \; M_o^T \; F_{11}^T \; F_{12}^T \cdots F_{1n_1}^T \; F_{21}^T \; F_{22}^T \cdots F_{2n_2}^T \cdots F_{N1}^T \; F_{N2}^T \cdots F_{Nn_N}^T]^T \tag{28}$$

is recognized as the actual control vector, and

$$d(t) = \begin{bmatrix} \sum_{e=1}^{N} E_e^T(\tilde{S}_e\dot{\omega}_e + \tilde{\omega}_e\tilde{S}_e\omega_e) \\ \sum_{e=1}^{N} [\tilde{r}_{oe}E_e^T(\tilde{S}_e\dot{\omega}_e + \tilde{\omega}_e\tilde{S}_e\omega_e) - E_e^T(I_e\dot{\omega}_e + \tilde{\omega}_e I_e\omega_e)] \\ -\tilde{\Phi}_1^T\dot{\omega}_1 + \int_{m_1} \Phi_1^T\tilde{\omega}_1\tilde{r}_1\omega_1 \, \mathrm{d}m_1 \\ \vdots \\ -\tilde{\Phi}_N^T\dot{\omega}_N + \int_{m_N} \Phi_N^T\tilde{\omega}_N\tilde{r}_N\omega_N \, \mathrm{d}m_N \end{bmatrix} \tag{29}$$

is an inertial disturbance vector

III. Maneuvering and Control

The maneuver consists of retargeting antennas so as to point in given directions in the inertial space. By stabilizing the platform in an inertial space, the task reduces to reorienting the antennas relative to the platform. For a minimum-time maneuver, the control law is bang-bang, which implies that the angular acceleration of an antenna relative to the platform is constant, with the sign changing at half the maneuver period. Ideally, the maneuver should not cause elastic deformations in the flexible appendages. This is likely to require a long maneuver time, which is in conflict with the minimum-time requirement. Hence, elastic deformations are likely to occur, which in turn implies perturbation of the platform from a fixed position in the inertial space.

The motion of the system is governed by Eq. (22). The system is characterized by two factors that distinguish it from most commonly encountered systems: it is time-varying and it is subjected to persistent disturbances. Both factors arise from the retargeting maneuver angular velocities ω_e, angular accelerations $\dot{\omega}_e$, and the matrices E_e of direction cosines ($e = 1,2,\ldots,N$), all quantities being known functions of time. Consistent with the nature of the system, we consider a control consisting of two parts: one part counteracting the persistent disturbances and a second part driving the state to zero. The control counteracting the persistent disturbances is open-loop, and the regulator is closed-loop. Hence, we assume a control in the form of the sum

$$f(t) = f_o(t) + f_c(t) \tag{30}$$

so that, inserting Eq. (30) into Eq. (22), we obtain

$$\dot{x}(t) = A(t)x(t) + B(t)[f_o(t) + f_c(t)] + D(t)d(t) \tag{31}$$

The open-loop control is assumed to satisfy

$$B(t)f_o(t) + D(t)d(t) = \mathbf{0} \tag{32}$$

so that, recalling Eqs. (23b) and (23c), we obtain

$$f_o(t) = -[B^*(t)]^{\dagger}d(t) \tag{33}$$

where

$$(B^*)^{\dagger} = [(B^*)^T B^*]^{-1}(B^*)^T \tag{34}$$

is the pseudoinverse of B^*. From the nature of the matrix B^*, Eqs. (26) and (27), it is clear that $(B^*)^{\dagger}$ exists, provided that the actuators are placed so that the matrices $\Phi(r_{ei})$ have full rank.

The closed-loop control is assumed to be optimal, in the sense that it minimizes the performance index

$$J = \frac{1}{2}x^T(t_f)Hx(t_f) + \frac{1}{2}\int_{t_o}^{t_f}(x^TQx + f_c^TRf_c)\,\mathrm{d}t \tag{35}$$

where t_o and t_f are the initial and final time, respectively, and H, Q, and R are coefficient matrices to be selected by the analyst.[7] Minimization of J yields the optimal control law

$$f = -R^{-1}B^Tpx \tag{36}$$

where P is an optimal control gain matrix satisfying the matrix Riccati equation

$$\dot{P} = -PA - A^TP - Q + PBR^{-1}B^TP \tag{37a}$$

$$P(t_f) = H \tag{37b}$$

The closed-loop state equation is obtained by inserting Eqs. (33) and (36) into Eq. (31), with the result

$$\dot{x}(t) = A_c(t)x(t) + D_c(t)d(t) \tag{38}$$

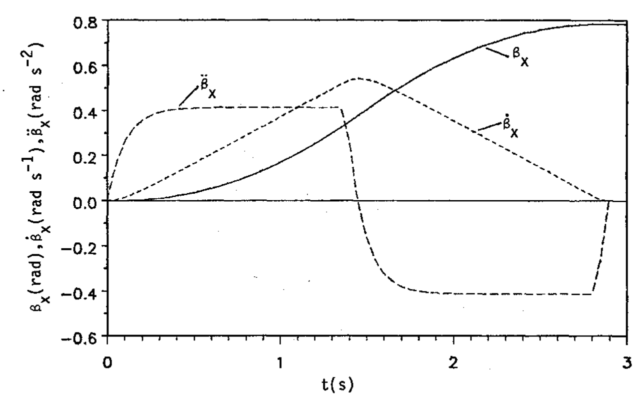

Fig. 4 Time history of the appendage maneuver.

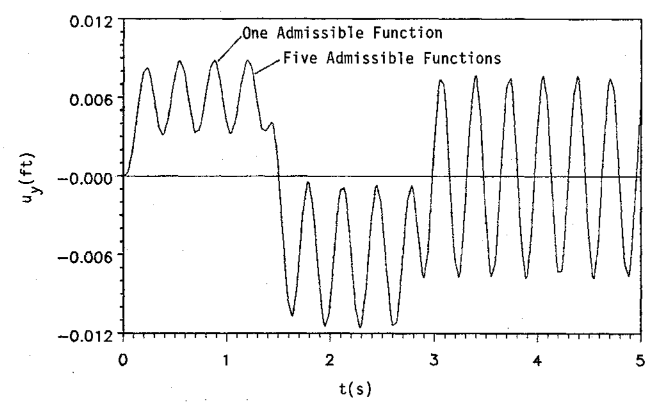

Fig. 5 Time history of the uncontrolled tip elastic displacement.

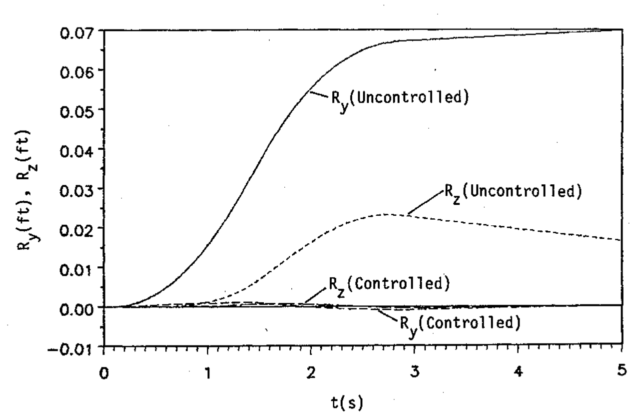

Fig. 6 Time history of the rigid-body translations ($Q = 100\ I$, $R = 0.001\ I$).

where

$$A_c = A - BR^{-1}B^TP = \left[\begin{array}{c|c} 0 & I \\ \hline -M^{-1}[K + B^*R^{-1}(M^{-1}B^*)^TP_{21}] & -M^{-1}[G + B^*R^{-1}(M^{-1}B^*)^TP_{22}] \end{array}\right] \tag{39a}$$

in which P_{21} and P_{22} are submatrices of P, and

$$D_c = D - B(B^*)^\dagger = \left[\begin{array}{c} 0 \\ \hline M^{-1}\{I - B^*[(B^*)^TB^*]^{-1}(B^*)^T\} \end{array}\right] \tag{39b}$$

Clearly, how well the control is able to drive the elastic vibration and the deviations of the platform from equilibrium relative to the inertial space to zero depends to a large extent on how close D_c is to the null matrix, which in turn depends on how close the matrix B^* is to a square matrix. The latter depends on the number of actuators.

IV. Numerical Example

The preceding developments have been applied to a spacecraft consisting of a rigid platform with a single flexible appendage in the form of a beam (Fig. 3). The maneuver consists of slewing the beam relative to the platform through a 45-deg angle about the x axis, so that $\omega_e = [\dot\beta_x \; 0 \; 0]^T$. The time history of the angular acceleration $\ddot\beta_x$ is a smoothed bang-bang, where the smoothing was used to reduce the elastic deformations of the appendage. Plots of the angular acceleration $\ddot\beta_x$ vs angular velocity $\dot\beta_x$, and angular displacement β_x vs time are shown in Fig. 4. The elastic motion consists of bending vibration in the x and y directions, with the vibration in the z direction being identically equal to zero. The vibration was represented by five admissible functions in each direction, so that the matrix Φ_e in Eq. (5) is 3×10 and the vector q_e is a ten-dimensional vector. The admissible functions have the expressions

$$\phi_{xj} = -(\cos\beta_j z - \cos\beta_j z) + C_j(\sin\beta_j z - \sinh\beta_j z) \qquad j = 1,2,\ldots,5 \tag{40}$$

which are recognized as cantilver modes.[8] The admissible functions ϕ_{yj} ($j = 6,7,\ldots 10$) have exactly the same expressions. The coefficients in Eq. (40) have the values $C_j = 0.7341$, 1.0185, 0.9992, 1, 1, and the arguments of the trigonometic and hyperbolic functions can be obtained from $\beta_j \ell_e = 1.8751$, 4.6941, 7.8548, 10.9955, 14.1372, where ℓ_e is the length of the beam. The mass matrix [Eq. (9g)] and stiffness matrix [Eq. (10)] are 10×10 and have the block-diagonal form

$$M_e = \left[\begin{array}{c|c} M_{e11} & 0 \\ \hline 0 & M_{e22} \end{array}\right] \tag{41a}$$

$$K_e = \left[\begin{array}{c|c} K_{e11} & 0 \\ \hline 0 & K_{e22} \end{array}\right] \tag{41b}$$

where

$$M_{e11} = M_{e22} = [m_e \delta_{ij}] \tag{42a}$$

$$K_{e11} = K_{e22} = \frac{EI_e}{\ell_e^3}(\beta_i \ell_e)^2(\beta_j \ell_e)^2 \delta_{ij}, \quad i,j = 1,2,\ldots,5 \tag{42b}$$

Moreover, the matrices $\bar\Phi_e$ and $\tilde\Phi_e$ given by Eqs. (9h) and (9i), respectively, are 3×10 and have the form

$$\bar\Phi_e = \begin{bmatrix} \bar\phi_e & 0 \\ 0 & \bar\phi_e \\ 0 & 0 \end{bmatrix} \tag{43a}$$

$$\tilde\Phi_e = \begin{bmatrix} 0 & -\tilde\phi_e \\ \tilde\phi_e & 0 \\ 0 & 0 \end{bmatrix} \tag{43b}$$

where $\bar\phi_e = m_e[0.783 \;\; 0.434 \;\; 0.254 \;\; 0.182 \;\; 0.141]$ and $\tilde\phi_e = m_e \ell_e \, [0.569 \; 0.091 \; 0.032 \; 0.017 \; 0.010]$. Other numerical values used are

$$m_r = 15.6 \text{ slugs}, \quad m_e = 0.15 \text{ slugs}$$

$$S_e = [0 \;\; 0 \;\; 0.375]^T \text{ slugs} \cdot \text{ft}$$

$$I_r = \begin{bmatrix} 13 & 0 & 0 \\ 0 & 48 & 0 \\ 0 & 0 & 59 \end{bmatrix} \text{ slugs} \cdot \text{ft}^2$$

$$I_e = \begin{bmatrix} 1.25 & 0 & 0 \\ 0 & 1.25 & 0 \\ 0 & 0 & 0 \end{bmatrix} \text{ slugs} \cdot \text{ft}^2$$

$$\ell_e = 5 \text{ ft}, \quad EI_e = 500 \text{ lb} \cdot \text{ft}^2, \quad r_{oe} = [0 \;\; 0 \;\; 0.4]^T \text{ ft}$$

Figure 5 shows the time history of the tip elastic displacement of the appendage in the absence of control. Although five admissible functions were used to represent the elastic

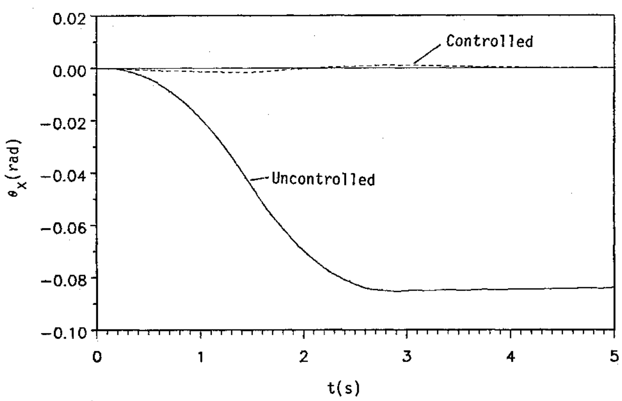

Fig. 7 Time history of the rigid-body rotation ($Q = 100 \; I$, $R = 0.001 \; I$).

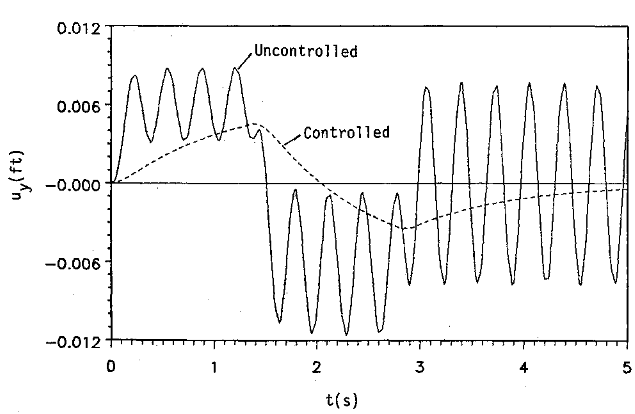

Fig. 8 Time history of the tip elastic displacement without and with control ($Q = 100 \; I$, $R = 0.001 \; I$).

displacements, sufficient accuracy can be obtained with a single admissible function alone. Indeed, there is no discernible difference in the open-loop response using one or five admissible functions, as can be verified from Fig. 5.

Figures 6 and 7 show time histories of the rigid-body translations and rotation of the platform during the maneuver, respectively, without and with control. Finally, Fig. 8 shows the tip elastic displacement of the appendage during the maneuver, without and with control. The controls were implemented by six actuators mounted on the rigid platform and two actuators each for the x and y directions and located on the appendage at $z = \ell_e/2$ and $z = \ell_e$.

For the values of the parameters chosen, the time-varying terms in the coefficient matrices turned out to be small compared to the constant terms. In view of this, the control gains were computed as if the system were time invariant. They were obtained by solving the steady-state Riccati equation in conjunction with Potter's method.[9] The coefficient matrices A and B used in the solution were according to the premaneuver state. Moreover, we chose the performance index coefficient matrices $H=0$, $Q=100\ I$, and $R=0.001\ I$, where I is the identity matrix. This assumes large final time t_f. It should be stressed once again that the time-invariant system was used only for computing the control gains, and the closed-loop response plots were obtained by considering the actual time-varying system, as described by Eq. (38).

V. Summary and Conclusions

The equations describing the motion of a spacecraft consisting of a rigid platform and retargeting flexible antennas can be derived most conveniently by means of a Lagrangian approach in terms of quasicoordinates. The strategy used consists of stabilizing the platform relative to an inertial space and maneuvering the antennas relative to the platform. In general, the equations are nonlinear and time varying. In the case in which the inertia of the antennas is small relative to that of the spacecraft, the equations can be linearized, although they remain time-varying. In addition, the equations contain persistent disturbances due to inertial loading.

The control can be divided into two parts, the first counteracting the persistent disturbances and the second providing regulation of the system. The state subject to regulation consists of the deviations of the platform from equilibrium relative to the inertial space and the elastic motions of the appendages. The feedback control gains for the regulator can be made optimal by minimizing a certain performance measure.

In the case investigated the time-varying terms were relatively small so that the control gains were computed on the basis of the time-invariant system obtained by ignoring the time-varying terms. However, in determining the response, the resulting control forces were applied to the actual time-varying system, thus validating the efficacy of the control design.

Acknowledgments

This research was sponsored in part by the U.S. Air Force Aeronautical Systems Division and Air Force Office of Scientific Research under Research Grant F33615-86-C-3233, monitored by Drs. V. B. Venkayya and A. K. Amos, whose support is greatly appreciated.

References

[1]Turner, J. D. and Junkins, J. L., "Optimal Large-Angle Single-Axis Rotational Maneuvers of Flexible Spacecraft," *Journal of Guidance and Control*, Vol. 3, Nov.–Dec. 1980, pp. 578–585.

[2]Breakwell, J. A., "Optimal Feedback Slewing of Flexible Spacecraft," *Journal of Guidance and Control*, Vol. 4, Sept.–Oct. 1981, pp. 472–479.

[3]Meirovitch, L. and Quinn, R. D., "Maneuvering and Vibration Control of Flexible Spacecraft," *Journal of Astronautical Sciences*, Vol. 35, No. 3, July–Sept. 1987, pp. 301–328.

[4]Quinn, R. D. and Meirovitch, L., "Maneuvering and Vibration Control of SCOLE," *Journal of Guidance, Control, and Dynamics*, Vol. 11, Nov.–Dec. 1988, pp. 542–442.

[5]Meirovitch, L. and Sharony, Y., "Optimal Vibration Control of a Flexible Spacecraft During a Minimum-Time Maneuver," *Proceedings of the Sixth VPI&SU/AIAA Symposium on Dynamics and Control of Large Structures*, Virginia Polytechnic Inst. and State Univ., Blacksburg, VA, 1987, pp. 579–601.

[6]Meirovitch, L., "State Equations of Motion for Flexible Bodies in Terms of Quasi-Coordinates," *Proceedings of the IUTAM/IFAC Symposium on Dynamics of Controlled Mechanical Systems*, Zurich, Switzerland, May–June 1988.

[7]Athans, M. and Falb, P. L., *Optimal Control*, McGraw-Hill, New York, 1966.

[8]Meirovitch, L., *Computational Methods in Structural Dynamics*, Sijthoff & Nordhoff, The Netherlands, 1980.

[9]Potter, J. E., "Matrix Quadratic Solutions," *SIAM Journal of Applied Mathematics*, Vol. 14, No. 3, 1966, pp. 496–501.